Title: Single voxel autocorrelation reflects hippocampal function in temporal lobe epilepsy

Authors: Nichole R. Bouffard[1,2], Sam Audrain[1,3], Ali M. Golestani[4,5], Morgan D. Barense[1,2], Morris Moscovitch[1,2], & Mary Pat McAndrews[1,3]

Affiliations:

[1]Department of Psychology, University of Toronto, Toronto, Ontario, Canada

[2]Rotman Research Institute, Baycrest Health Sciences, North York, Ontario, Canada

[3]Division of Clinical and Computational Neuroscience, Krembil Research Institute, University Health Network, Toronto, Ontario, Canada

[4]Department of Physics and Astronomy, University of Calgary, Alberta, Canada

[5]Hotchkiss Brain Institute, University of Calgary, Calgary, Alberta

Corresponding author: Nichole R. Bouffard, Email: nichole.bouffard@mail.utoronto.ca

Abstract

We have previously shown that analyses of autocorrelation of BOLD signal applied to single voxels in healthy controls can identify gradients of temporal dynamics throughout the hippocampal long-axis that are related to behavior. A question that remains is how changes in functional and structural integrity in the brain affect single voxel autocorrelation. In this study we investigate how hippocampal autocorrelation is affected by structural and functional hippocampal dysfunction by investigating a population of patients with unilateral temporal lobe epilepsy (TLE). Many patients with TLE have mesial temporal sclerosis (MTS), characterized by scarring and neuronal loss particularly in the anterior hippocampus. Here we compared patients with left and right TLE, some with and without MTS, to healthy controls. We applied our single voxel autocorrelation method and data-driven clustering approach to segment the hippocampus based on the autocorrelation. We found that patients with left TLE had slower signal dynamics (i.e., higher autocorrelation) compared to controls, particularly in the anterior-medial portion of the hippocampus. This was true for both the epileptogenic and non-epileptogenic hemispheres. We also evaluated the extent of cluster preservation (i.e., spatial overlap with controls) of patient autocorrelation clusters and the relationship to verbal and visuospatial memory. We found that patients with greater cluster preservation in the anterior-medial hippocampus had better memory performance. Surprisingly, we did not find any effect of MTS on single voxel autocorrelation, despite the structural changes associated with the condition. These results suggest that single voxel autocorrelation may be related to functional, rather than structural, integrity.

Keywords: hippocampus, autocorrelation, temporal lobe epilepsy, memory, mesial temporal sclerosis

1. Introduction

Human functional MRI is a powerful neuroimaging tool that has enabled us to observe in-vivo fluctuations of brain activity over time. Recently our lab has developed an fMRI analytic technique that allows us to measure dynamics in the BOLD signal over time in single voxels. Single voxel autocorrelation is the lagged autocorrelation of individual voxels, a measure of how similar a voxel's activity is to itself over time (Bouffard, Golestani et al., 2023; Coughlan et al., 2023). In healthy populations, single voxel autocorrelation is thought to reflect underlying neuronal dynamics, where high autocorrelation indicates slow fluctuations in neural activity and low autocorrelation indicates rapid fluctuations in neural activity. Prior work from our lab examined the hippocampus and found anterior-posterior and medial-lateral gradients of single voxel autocorrelation that were related to behavior in a navigation task (Bouffard, Golestani et al., 2023). Gradients of single voxel autocorrelation, therefore, may be an important property of a healthy functioning brain and might be the neural mechanism underlying cognitive processes in the hippocampus. Disruption of hippocampal autocorrelation gradients could have consequences for behavior, but it is still unclear how the single voxel autocorrelation in the hippocampus is affected in cases of hippocampal dysfunction and memory impairment. In this study we sought to add to this literature by investigating a population with well characterized structural and functional hippocampal dysfunction: patients with unilateral temporal lobe epilepsy (TLE). We examined the influence of medial temporal lobe damage on single voxel autocorrelation and uncovered how the spatial organization of single voxel autocorrelation is related to memory.

Temporal lobe epilepsy is the most common type of drug-resistant epilepsy in adults, and is frequently associated with structural abnormalities in the hippocampus (Coras & Blümcke, 2015). This damage, which is diagnosed as mesial temporal sclerosis (MTS), can be observed on MRI as both decreased volume and abnormal signal from mesial temporal structures (Jackson et al., 1990; Kuzniecky et al., 1997). Fifty percent of patients with TLE are diagnosed with MTS, and the damage is usually located in the anterior hippocampus (Bernasconi et al., 2003; Bernhardt et al., 2016; Kuzniecky et al., 1997; Thom et al., 2012). We reasoned that the structural changes in MTS would be reflected in changes in single voxel autocorrelation and/or the organization of single voxel autocorrelation throughout the hippocampus relative to healthy controls. In addition to structural changes, unilateral TLE is also associated with decreased memory performance, where deficits in verbal memory are related to TLE in the left temporal lobe and deficits in visuospatial memory are related to TLE in the right temporal lobe (Kelley et al., 1998; Kim et al., 2003; St-Laurent et al., 2014). If single voxel autocorrelation is related to memory, then changes in single voxel autocorrelation might be related to verbal and visuospatial memory performance in patients with TLE.

Other studies have investigated the changes in temporal dynamics associated with TLE using different approaches. There are several reports of elevated temporal autocorrelation and reduced complexity of EEG signals of patients with TLE in the epileptogenic hippocampus compared with the healthy, contralateral hippocampus, which has been observed both at rest (Monto et al., 2007; Parish et al., 2004) and during cognitive tasks (Protzner et al., 2010). A recent study using fMRI found a decrease in hippocampal autocorrelation of the BOLD signal (using a different method

than the one used here) suggesting more rapid dynamics in the hippocampus and more widespread areas of cortex bilaterally in TLE (Xie et al., 2023). These prior studies examined the temporal dynamics of the hippocampus as a whole and have not examined the organization of autocorrelation along the anterior-posterior and medial-lateral axes of the hippocampus in patients with TLE. Our past work suggests that the gradient organization of single voxel autocorrelation is a critical component in the relationship between single voxel autocorrelation and behavior, therefore an aim of the current study was to examine how location-dependent single voxel autocorrelation is affected by TLE and whether it is related to memory performance.

In the healthy hippocampus, single voxel autocorrelation follows a gradient from high-to-low along the anterior-posterior and medial-lateral axes (Bouffard, Golestani et al., 2023; Coughlan et al., 2023; Raut et al., 2020). These continuous gradients can be segmented into distinct clusters based on the autocorrelation of individual voxels and result in three segments: an anterior-medial cluster of high autocorrelation voxels, an intermediate cluster, and a posterior-lateral cluster of low autocorrelation voxels (Bouffard, Golestani et al., 2023; Coughlan et al., 2023). Our past work used a data-driven clustering approach and found that changes in single voxel autocorrelation, specifically in the anterior-medial cluster, were related to changes in navigation difficulty. This suggests that hippocampal autocorrelation might be related to behavior in a location-dependent manner, where slow changing dynamics in the anterior-medial hippocampus are particularly important for certain types of navigation. The spatial organization of autocorrelation clusters therefore might be important for healthy hippocampal function and it remains unknown whether the spatial organization of

autocorrelation clusters is altered by hippocampal damage and whether changes in autocorrelation clustering relate to memory. An aim of the current study, therefore, was to evaluate changes in spatial organization of autocorrelation clusters by quantifying the spatial overlap of clusters between patients and controls and to test whether this overlap was related to memory performance.

In the current study, we used resting-state fMRI from patients with unilateral left or right TLE and age-matched controls to examine single voxel autocorrelation and autocorrelation clustering in the hippocampus. First, we investigated whether single voxel autocorrelation and autocorrelation clusters differed between patients and controls, with the prediction that the average single voxel autocorrelation within the clusters of patients and controls would differ, especially within the anterior cluster of patients with MTS due to the presence of structural damage. We then correlated the average single voxel autocorrelation with memory performance on neuropsychological tests. To determine whether the organization of single voxel autocorrelation along the long-axis is related to memory, we computed a metric of cluster preservation, or the degree to which individual patient clusters spatially overlap with control clusters, and correlated this with verbal and visuospatial memory. We predicted that patients with greater cluster preservation would also have better memory performance. This work advances our understanding of the different properties of hippocampal signaling dynamics that are measured with single voxel autocorrelation and how they relate to memory.

2. Materials and Methods

2.1 Participants

Forty-nine adult patients with pharmacologically intractable unilateral TLE were recruited from the Epilepsy Clinic at Toronto Western Hospital. Twenty-three patients presented with left TLE (LTLE) (Female = 15, Mean Age = 37.43, SD = 12.46) and 26 presented with right TLE (RTLE) (Female = 9, Mean Age = 36.80, SD = 14.12). Continuous recording of scalp EEG and video monitoring during an inpatient evaluation in our epilepsy monitoring unit were used to determine seizure focus. MTS was diagnosed based on designations by a neuroradiologist from patients' T1- and T2-weighted anatomic scans. Thirteen patients with LTLE had MTS and 16 patients with RTLE had MTS. Two individuals (1 LTLE, 1 RTLE) did not have confirmed MTS but had hippocampal abnormalities. There was also one patient who had RTLE but MTS in the left hemisphere. Twenty-nine neurologically healthy control participants (Female = 16, Mean Age = 34, SD = 10.81) were recruited to serve as comparison for our patient sample. All controls gave prospective written informed consent. Prospective written informed consent was obtained from a subset of the patient group, while permission for retrospective analysis of clinical data (both neuropsychological and resting-state fMRI) was obtained from the University Health Network Ethics Board for a group of participants who were scanned prior to the current ethics protocol implementation.

2.2 Neuropsychological Testing

A comprehensive neuropsychological battery was administered to patients that included assessment of intelligence, learning/memory, processing speed, and verbal and visuospatial functioning. The battery included the following measures: Wechsler

Abbreviated Scale of Intelligence, Warrington recognition memory test for faces, Rey visual design learning test, spatial conditional associative learning test, Warrington recognition memory test for words, and Rey auditory verbal learning test. Summary memory scores were computed to capture a more reliable representation of core abilities than afforded by single test scores. We transformed the neuropsychological test scores into summary verbal and visuospatial scores using the previously estimated factor loadings from a principal components analysis following previous work from our group (see St-Laurent et al., 2014 for a full description of method). The visuospatial memory factor was primarily based on loadings from correct responses on the Warrington recognition memory test for faces (RMF), total recall across trials one through five on the Rey visual design learning test (RVDL), and number of trials to criterion for the conditional associative learning test (CAL). The verbal memory factor was based on loadings from correct responses on the Warrington recognition memory test for words (RMW), total recall (RAVLT-tot) over five study-test trials from the Rey auditory verbal learning test (RAVLT) and percent retention (RAVLT-ret) at 20-minute delay from the RAVLT.

2.3 MRI Acquisition

A high-resolution 3D anatomical scan was collected on a 3T Signa MR system (GE Medical Systems, Milwaukee, WI, USA) for each participant (T1- weighted sequence, FOV 220mm, 146 slices, flip angle = 12 degrees, 256x256 matrix, resulting in voxel size of 0.86 x 0.86 x 1.0). Six-minute resting state fMRI (T2∗-weighted) scans were acquired with an echo-planar pulse imaging (EPI) sequence (FOV 240mm, 28–32

slices depending on head size, TR = 2,000ms, TE = 25ms, 64 x 64 matrix, 3.75 x 3.75 x 5mm voxels, for 180 volumes). During resting state scans, participants were instructed to lie still, and “not to think about anything in particular,” with their eyes closed.

2.4 Functional MRI Pre-processing

Preprocessing was performed using SPM8 (http://www.fil.ion.ucl.ac.uk/spm/software/spm8), a toolbox running in MATLAB 2018a (Mathworks). Anatomical and functional images were reoriented so that the origin falls on the anterior commissure. The functional images were then corrected for slice-timing, realigned and unwarped, and then co-registered to the anatomical image. Anatomical images for each participant were segmented into gray matter, white matter and cerebral spinal fluid (CSF) and normalized into standard MNI space. Functional images were then normalized to standard space using the parameters from the anatomical transformation. The single voxel autocorrelation method involves analysis of individual voxels therefore no spatial smoothing was performed. Using the Conn toolbox (Whitfield-Gabrieli & Nieto-Castanon, 2012), a CompCor (Behzadi et al., 2007) was used to exclude measures of physiological noise by regressing out the top five components of a principal components analysis from eroded white matter and CSF masks produced from the SPM8 segmentation. Motion scrubbing using the ART function was also applied to reduce artefacts due to motion. Any timepoint that was 3 or more standard deviations from the mean global brain activation, more than 1mm of linear motion, or more than 0.05 radians rotation was regressed from the data. Low-pass temporal filtering was applied

before computing the single voxel autocorrelation to exclude high (>0.09Hz) frequency fluctuations. The filtered and corrected images were used for subsequent analyses.

2.5 Single voxel autocorrelation method

2.5.1 Computing single voxel autocorrelation

We used the single voxel autocorrelation method described by Bouffard, Golestani et al. (2023) and describe the method briefly here. Bilateral hippocampal masks were generated using the Harvard-Oxford Atlas in FSL. For each voxel, unbiased autocorrelation (as implemented in MATLAB xcorr cross-correlation function) was calculated. Specifically, the timecourse of a single voxel's activity was correlated with itself shifted by a temporal lag, the length of 1 TR (TR = 2000 ms). We repeated this process, shifting the timecourse forward by 1 lag (2000 ms) and correlating it with the original, non-shifted timecourse until a maximum temporal shift of 4 seconds was reached. We chose 4 seconds because it has been shown that the autocorrelation of the fMRI signal in the gray matter drops off after 4 seconds (Bollmann et al., 2018). The non-shifted timecourse was correlated with lag 1 (length of 1 TR) and with lag 2 (length of 2 TRs) (Figure 1A). The autocorrelation (AC) computed for each lag was stored in a vector. The autocorrelation vector contained 2 values (one single voxel autocorrelation value for each lag). This approach resulted in an autocorrelation vector for each voxel (Figure 1). The vectors were then used to compute autocorrelation clusters in the next step.

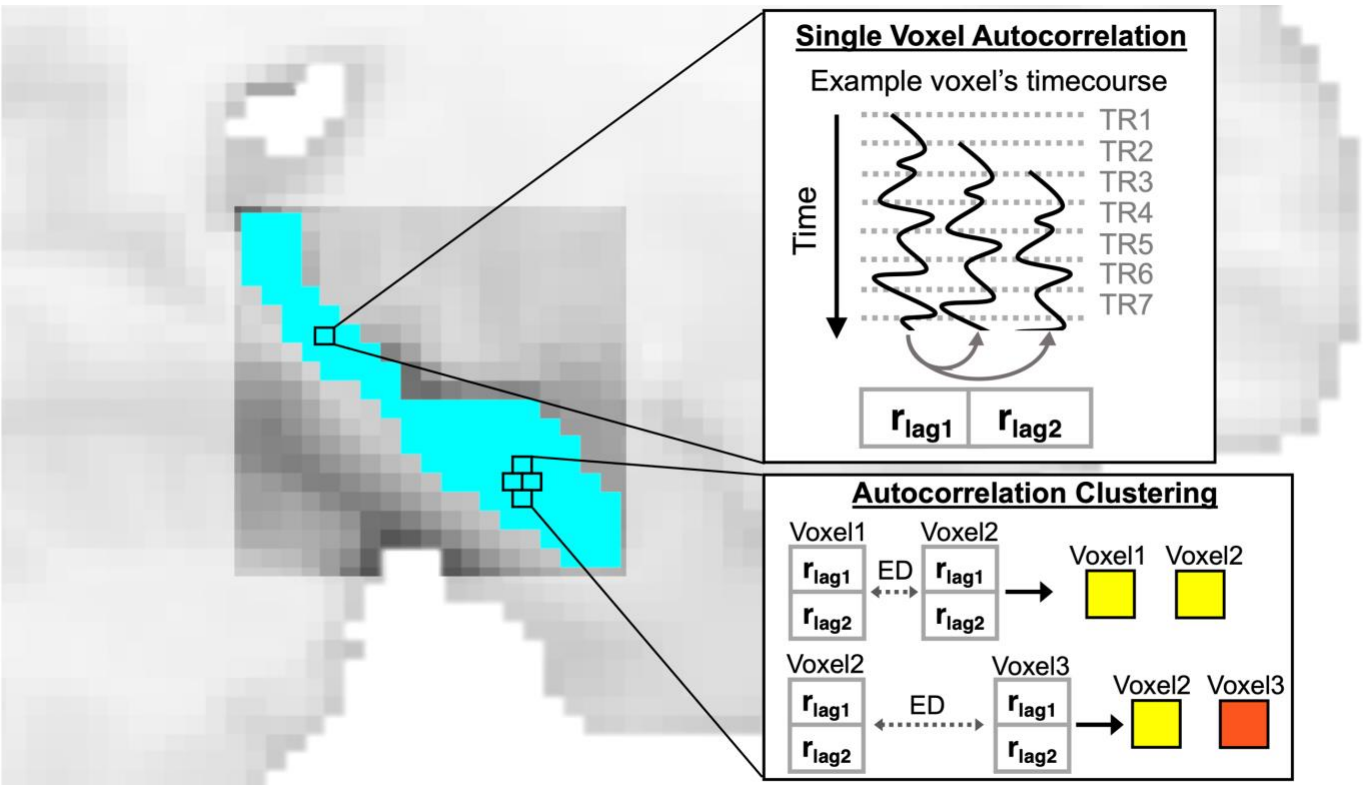

Figure 1. Single voxel autocorrelation method. For each voxel in the hippocampus, the time course of BOLD activity was successively temporally shifted by 1 TR and correlated with itself. This was repeated for a total shift of 4 seconds (i.e., 2 lags). This resulted in a vector of single voxel autocorrelation values, with each value corresponding to a different lagged correlation. **Autocorrelation clustering.** The single voxel autocorrelation vectors for every voxel were used to compute the autocorrelation clusters, where voxels were clustered based on the Euclidean distance (ED) of their single voxel autocorrelation vectors. Every voxel was assigned to a cluster and the total number of clusters was determined by the modularity optimization algorithm (i.e., number of clusters was not predetermined). Yellow and red voxels represent voxels that were assigned to the same (voxel 1 and 2) or different clusters (voxel 1 and 3). Clustering was performed at the individual participant level, and a separate cluster map was created for each individual and each hemisphere. Group-level cluster maps were created by averaging across individuals.

2.5.2 Autocorrelation Clustering

For the next step, the Euclidean distance between the single voxel autocorrelation vectors of each voxel pair in each mask was calculated to create a distance matrix. The distance matrix was first normalized (i.e., divided by the maximum value) and then subtracted from 1 to generate a similarity matrix ranging from 0 to 1. This similarity matrix was used to generate hippocampal clusters using the modularity optimization algorithm proposed by Blondel et al., (2008) and Wickramaarachchi et al., (2014). Unlike most other clustering methods, modularity optimization does not require a predesignated number of clusters and instead estimates the optimum number of clusters from data. An autocorrelation cluster map for left and right hippocampus was created for each individual. In addition to clustering at the individual level, group-level clusters were derived by averaging the similarity matrices of all participants. Group-level autocorrelation cluster maps were created for the Control, LTLE and RTLE groups (Figure 2). We computed reliability of autocorrelation clusters by computing the overlap of clusters with each group (Control, LTLE, RTLE). By comparing the spatial organization of clusters of individuals within the same group, we determined that the anterior-medial cluster and posterior-lateral cluster were the most reliable clusters, whereas the intermediate cluster was more variable across individuals and therefore less reliable. See Supplemental Materials for the detailed reliability analysis and Figure S1 for the reliability data of each cluster.

2.6 Cluster preservation: Overlap of individual autocorrelation clusters with group-level Control clusters

To compute cluster preservation, or the overlap of individual patient clusters with the group-averaged Control clusters, we measured the spatial overlap (Jaccard coefficient) between each patient's autocorrelation cluster map with the group-level average autocorrelation cluster map from the Control group. The Jaccard coefficient of regions A and B is defined as:

$$J(A,B) = \frac{|A \cap B|}{|A \cup B|}$$

Where $|A \cap B|$ is the number of common voxels in both A and B (intersection) and $|A \cup B|$ is the number of voxels in A and B combined (union). We calculated the Jaccard coefficient between each individual's autocorrelation cluster map and the group-level autocorrelation cluster map from Controls. We computed the Jaccard coefficient for each autocorrelation cluster separately.

High spatial overlap (i.e., large Jaccard coefficients) suggests greater spatial similarity/preservation of the spatial distribution of autocorrelation clusters relative to Controls. Low spatial overlap (i.e., small Jaccard coefficients) would suggest less spatial similarity/preservation of spatial distribution of autocorrelation clusters relative to Controls. For example, consider a voxel from the healthy control group that had high single voxel autocorrelation and was assigned to a specific cluster. In a patient, if that same voxel had a decrease in single voxel autocorrelation due to changes in the underlying dynamics, that voxel would now be assigned to a different cluster. This assignment would lead to changes in how the autocorrelation clusters are organized throughout the hippocampus of patients compared to controls.

To determine whether cluster preservation was related to memory, we correlated cluster preservation and patient neuropsychological test summary scores for verbal and

visuospatial memory. Left TLE is associated with deficits in verbal memory and right TLE is associated with deficits in visuospatial memory (Kim et al., 2003; St-Laurent et al., 2014). Therefore, we specifically correlated verbal memory scores with cluster preservation from LTLE patients and visuospatial memory scores with cluster preservation from RTLE patients.

3. Results

3.1 Single voxel autocorrelation clusters

We found that nearly every individual within the Control, LTLE, and RTLE groups had three hippocampal autocorrelation clusters in both the left and right hemispheres (Figure 2). There was one exception, a Control participant who only had two autocorrelation clusters in the right hemisphere, and we excluded this participant from further analyses. Consistent with prior work, we found one cluster in the posterior-lateral hippocampus, one cluster in the anterior-medial hippocampus, and an intermediate cluster (Figure 2). We also computed the size of each cluster (i.e., number of voxels assigned to each cluster). There were no significant differences in cluster size between Control, LTLE, and RTLE groups (See Supplemental Materials Table S1 for list of cluster sizes).

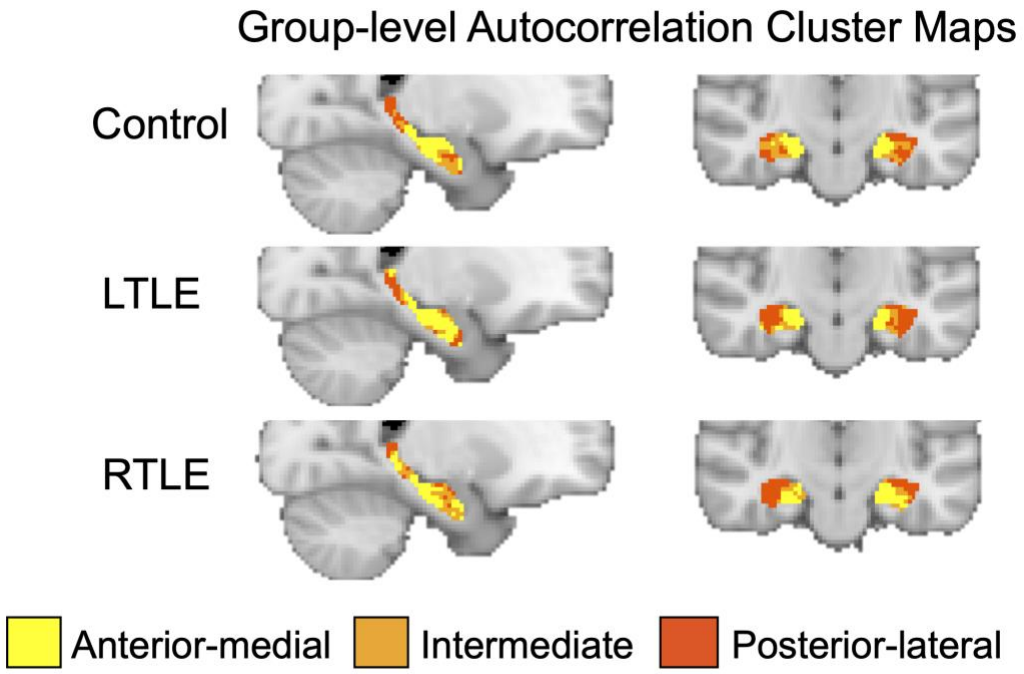

Figure 2. Group-level autocorrelation clusters. Hippocampal voxels were clustered based on the similarity (Euclidean distance) of single voxel autocorrelation vectors, resulting in one cluster in the anterior-medial hippocampus (yellow) associated with high autocorrelation values, one in the posterior-lateral hippocampus (red) associated with low autocorrelation values, and one cluster in the intermediate hippocampus (orange) in between the anterior-medial and posterior-lateral clusters.

For the following analyses, we computed the average single voxel autocorrelation in each of the three clusters per participant. We ran a linear mixed effects model with cluster (anterior-medial, intermediate, posterior-lateral), group (LTLE (N=23), RTLE (N=26), Control (N=28)), and hemisphere (left, right) as predictors, including participant as the random intercept in the random effects term. We found a main effect of cluster ($F(2,370) = 378.25$, $p < 0.001$) and a main effect of group ($F(2,74)=5.15$, $p < .01$). There was no effect of hemisphere ($F(1,370)= 0.78$, $p = 0.37$). For the post hoc analysis of the main effects, we used the Kenward-Roger method to

calculate the degrees of freedom and the Tukey method to correct for multiple comparisons. Post-hoc investigations of the main effect of cluster revealed that the anterior-medial cluster had the highest single voxel autocorrelation, followed by the intermediate cluster, and lastly the posterior-lateral cluster, which had the lowest single voxel autocorrelation (anterior-medial > intermediate: $t(370)= 20.95$, $p < 0.001$; anterior-medial > posterior-lateral: $t(370) = 25.91$, $p < 0.001$; intermediate > posterior-lateral: $t(370) = 4.96$, $p < 0.001$) (Figure 3A). See Supplemental Materials Table S2 for average autocorrelation values per cluster. Post-hoc analysis of the main effect of group revealed that individuals with LTLE had higher single voxel autocorrelation values than those with RTLE or Controls (LTLE > RTLE: $t(74) = 2.76$, $p < 0.05$; LTLE > Controls: $t(74) = 2.87$, $p < 0.05$). There was no difference in single voxel autocorrelation between the RTLE and Control groups ($t(74) = 0.06$, $p=0.99$).

We also found a significant cluster x group interaction ($F(4,370)=8.95$, $p < 0.001$). Post-hoc analysis revealed that this interaction was driven by higher single voxel autocorrelation in the anterior-medial cluster in LTLE patients compared to RTLE and Controls (LTLE > RTLE: $t(134) = 5.35$, $p < 0.001$; LTLE > Controls: $t(134) = 4.61$, $p < 0.001$) (Figure 3A). Notably, this was true for both the epileptogenic (left) and non-epileptogenic (right) hippocampi.

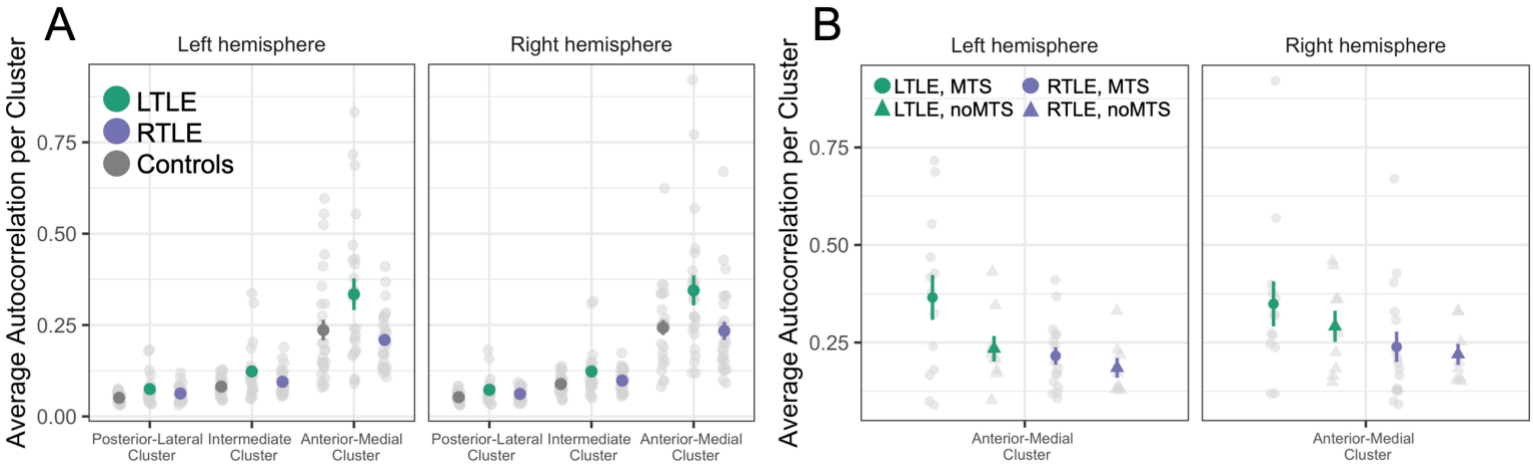

Figure 3. A) Average autocorrelation per cluster by group. The single voxel autocorrelation was averaged across voxels within each of the autocorrelation clusters from individuals in each of the three groups: Controls (gray), LTLE (green), and RTLE (purple). **B) Average autocorrelation in the anterior-medial hippocampal cluster by group and MTS status.** The average single voxel autocorrelation in just the anterior-medial cluster for LTLE and RTLE patients. Individuals are grouped by whether they had confirmed hippocampal mesial temporal sclerosis (MTS), resulting in four groups: LTLE with MTS (green circle), LTLE with noMTS (green triangle), RTLE with MTS (purple circle), and RTLE with noMTS (purple triangle).

These findings are consistent with our prior work in healthy individuals which has shown that clusters located in the anterior-medial hippocampus are associated with higher autocorrelation values compared to clusters in the posterior-lateral hippocampus. We predicted that both LTLE and RTLE groups would differ from Control and that within patients there would be a difference between affected and healthy hippocampi. In contrast, only the LTLE group had higher single voxel autocorrelation than controls, and that was seen in both left and right anterior-medial clusters.

In past work, the intermediate cluster has been shown to have low reliability within participants and includes significantly fewer voxels compared to the anterior-

medial and posterior-lateral clusters (Bouffard, Golestani et al., 2023; Coughlan et al., 2023). Here we again replicate this finding and found that the intermediate cluster had low reliability (See Supplemental Materials Figure S1) and was the smallest cluster (See Supplemental Materials Table S1 for list of cluster sizes). Therefore, for the rest of the analyses in the paper we chose to exclude it and only focus on the anterior-medial and posterior-lateral clusters.

3.1.1. Effect of Mesial Temporal Sclerosis (MTS) on single voxel autocorrelation

We predicted that hippocampal autocorrelation in patients with MTS would be different compared to patients without MTS in the affected hippocampus. Given the loss of neurons and associated gliosis is typically located in the anterior hippocampus (based off radiology examinations), we restricted our analyses to the cluster located in the anterior-medial hippocampus, as we predicted it would be more affected than the other clusters. We ran a linear mixed effects model on the average single voxel autocorrelation in the anterior-medial cluster for the LTLE and RTLE groups. We included MTS (MTS, noMTS), group (LTLE, RTLE), and hemisphere (left, right) as predictors. Note, there were 2 people (1 LTLE, 1 RTLE) who did not have confirmed MTS but had possible hippocampal abnormalities. Because we were not sure whether these participants had MTS, we excluded them from this analysis. There was also one participant who had RTLE but MTS in the left hemisphere, so we excluded that individual from this analysis. With these exclusions, the number of participants included in the following analyses was LTLE (N=22) and RTLE (N=24).

As above, we found a significant effect of group ($F(1,42) = 5.58$, $p < 0.05$), with the LTLE group demonstrating higher single voxel autocorrelation compared to the

RTLE ($t(42) = 2.36$, $p < 0.05$) (Figure 3B). Critically, we did not find an effect of MTS ($F(1,42) = 2.20$, $p = .146$) or any other significant effects or interactions. Nonetheless, individuals with confirmed MTS in the LTLE group had numerically higher single voxel autocorrelation in the affected hemisphere (left) than individuals without MTS. Given our predictions that MTS would affect single voxel autocorrelation, we tested this relationship directly with an independent samples t-test and found marginally higher single voxel autocorrelation in the MTS group compared to those without MTS ($t(18.16) = 1.98$, $p = 0.06$). The lack of a reliable effect of MTS suggests that the average single voxel autocorrelation is not dramatically affected by structural changes caused by MTS.

3.1.2. Relationship of single voxel autocorrelation to memory

To determine whether autocorrelation was related to memory we calculated the Pearson's correlation between the average single voxel autocorrelation in each of the clusters with verbal memory and visuospatial memory scores. We did this for each hemisphere separately as the well-known lateralization of verbal memory in the left temporal lobe and nonverbal memory in the right temporal lobe led us to specific predictions (Kelley et al., 1998; Kim et al., 2003; St-Laurent et al., 2014). We predicted that single voxel autocorrelation in the epileptogenic hemisphere of patients would be correlated with the corresponding dominant memory process attributed to that hemisphere (e.g., verbal memory in LTLE and visuospatial memory in RTLE). Note, one patient from the RTLE group had to be excluded from this analysis because we did not have all the relevant neuropsychological test measures for PCA. With this exclusion, the number of participants included in this analysis was LTLE (N=23) and RTLE (N=25). We

did not find any significant correlations between average single voxel autocorrelation and verbal memory in LTLE or visuospatial memory in RTLE, in either cluster (range of Rs: 0.067 - 0.34). See Supplemental Materials Table S3 for all R and p values.

3.2 Cluster preservation

We predicted that the spatial organization of autocorrelation throughout the hippocampus would be disrupted in cases of TLE. To test this prediction, we measured cluster preservation by comparing the spatial organization of individual patients' autocorrelation clusters to the spatial organization of group averaged Control clusters. We calculated the Jaccard coefficient, or the spatial overlap, between each patient's autocorrelation cluster map and compared it to the group-level autocorrelation cluster map for the Control group. The group-level autocorrelation cluster map was computed from Control participants (N=28) who all had three hippocampal clusters. A high Jaccard coefficient suggests that the spatial organization of autocorrelation clusters for an individual is comparable to the Control group and has high cluster preservation, whereas a low coefficient suggests the spatial organization has shifted compared to the normative group. See Supplemental Materials Table S4 for the Jaccard coefficients values for each autocorrelation cluster.

We conducted a linear mixed effects model on the Jaccard coefficients and included group (LTLE (N=23), RTLE (N=26), cluster (anterior-medial, posterior-lateral), and hemisphere (Left, Right) as the fixed effects predictors. We found a main effect of cluster ($F(1,141) = 34.36$, $p < 0.001$) and a main effect of hemisphere ($F(1,141) = 42.59$,

$p < 0.001$). We did not find a main effect of group ($p = 0.594$). We also found a significant cluster x hemisphere interaction ($F(1,141) = 8.87$, $p < 0.01$).

Post-hoc analysis of the main effect of cluster revealed that the anterior-medial cluster had lower cluster preservation, and therefore a greater deviation from the Control group, compared to the posterior-lateral cluster ($t(141) = 5.86$, $p < 0.001$). Post hoc analysis of the main effect of hemisphere revealed that the right hemisphere had greater cluster preservation than the left ($t(141) = 6.52$, $p < 001$). We did not find any differences in cluster preservation between LTLE and RTLE. Analysis of the cluster x hemisphere interaction revealed that the left anterior-medial cluster had lower cluster preservation compared to the right anterior-medial cluster ($t(141) = 6.72$, $p < .001$) and compared to both left ($t(141) = 6.25$, $p < .001$) and right ($t(141) = 8.75$, $p < .001$) posterior-lateral clusters. For the post hoc analysis of the main effects, we used the Kenward-Roger method to calculate the degrees of freedom and the Tukey method to correct for multiple comparisons.

3.2.1. Effect of MTS on cluster preservation

We predicted that patients with MTS would have decreased cluster preservation compared to those without MTS due to the structural changes caused by MTS. Because MTS typically affects the anterior hippocampus, we had specific predictions that the anterior-medial hippocampus would demonstrate more of a change in cluster preservation. To test this, we ran a linear mixed effects model on the Jaccard coefficients just in the anterior-medial cluster. We included MTS (MTS, noMTS), group (LTLE, RTLE), and hemisphere (left, right) as predictors. We again excluded the two people with possible abnormalities from this analysis and the one RTLE participant with

left MTS. With these exclusions, the number of participants included in the following analyses was LTLE (N=22) and RTLE (N=24). We did not find a significant effect of MTS ($F(1,42) = 0.00$, $p = 0.98$), nor did we find that MTS interacted with the other variables in the model. This result suggests that there was no difference in spatial organization of autocorrelation clusters between patients with MTS and without MTS.

3.2.2. Relationship of cluster preservation to memory

To understand whether the cluster preservation of autocorrelation clusters was related to memory, we computed the Pearson's correlation between cluster preservation and material-specific, lateralized memory scores (i.e., verbal memory scores for LTLE and visuospatial memory scores for RTLE). We focused our analyses on the anterior-medial cluster as that had shown the greatest deviation from the Control group. As above, one patient from the RTLE group had to be excluded from this analysis because we did not have their neuropsychology test scores. With this exclusion, the number of participants included in the following analyses was LTLE (N=23) and RTLE (N=25). We found that for LTLE individuals, better verbal memory scores were significantly correlated with greater cluster preservation in the anterior-medial cluster of the left hemisphere ($R = 0.46$, $p < 0.05$) (Figure 4). We did not find a significant correlation in the right hemisphere of the LTLE patients ($p = 0.64$). We found greater cluster preservation of the anterior-medial cluster in the right hippocampus for the RTLE group was correlated with better visuospatial memory ($R=0.44$, $p < 0.05$) (Figure 4). We did not find a significant correlation in the left hemisphere of the RTLE group ($p = 0.88$). Thus, there was a positive association between cluster preservation and material-

specific memory performance in the epileptogenic hippocampus of both LTLE and RTLE patients.

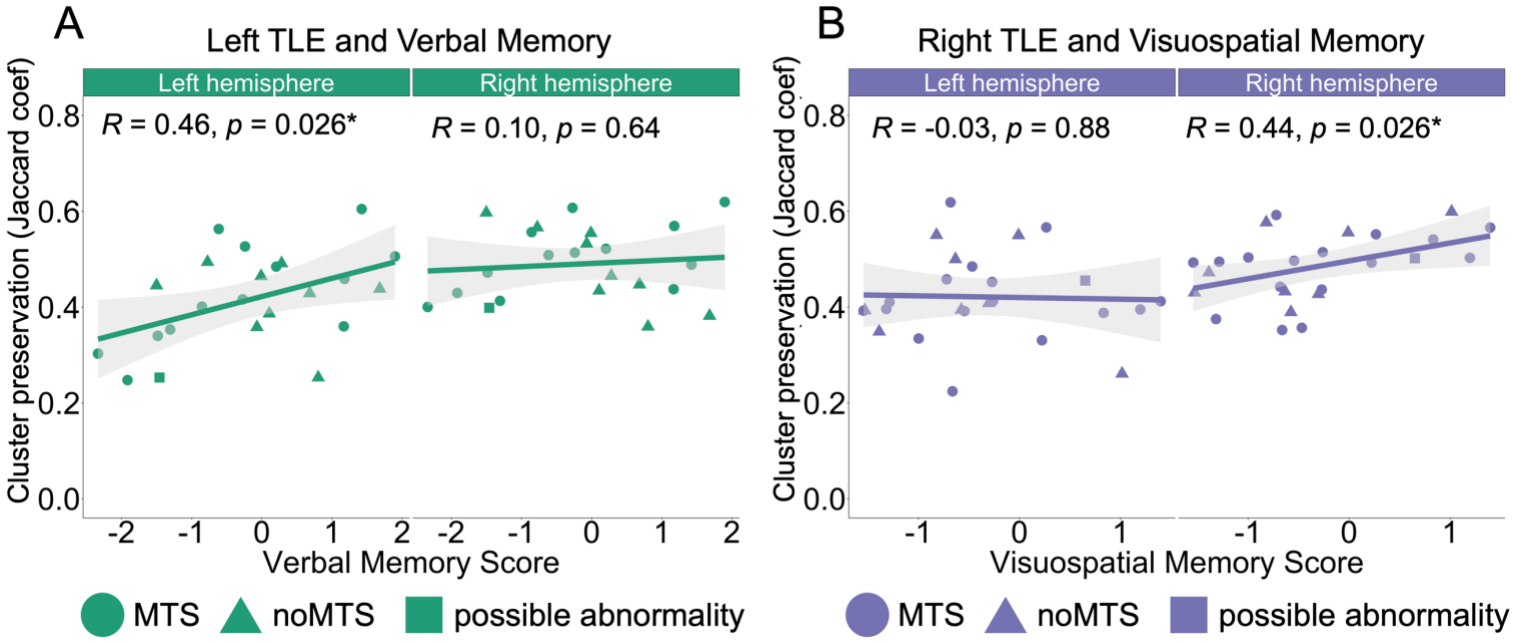

Figure 4. Cluster preservation in the anterior-medial cluster is correlated with memory. A. Verbal memory score correlated with cluster preservation (i.e., Jaccard coefficient) of the anterior-medial cluster in the left hemisphere and right hemisphere of LTLE individuals. The x-axis indicates verbal memory scores, where higher scores represent better performance. The y-axis indicates cluster preservation, where higher values represent greater similarity to Controls. LTLE patients with MTS (green circle), LTLE patients with noMTS (green triangle), and LTLE patients with possible hippocampal abnormality (green square). **B.** Visuospatial memory score correlated with cluster preservation of the anterior-medial cluster in the left and right hemisphere of individuals with RTLE. The x-axis indicates visuospatial memory scores, where higher scores represent better performance. The y-axis indicates cluster preservation, where higher values represent greater similarity to Controls. RTLE patients with MTS (purple circle), RTLE patients with noMTS (purple triangle), and RTLE patients with possible hippocampal abnormality (purple square).

4. Discussion

The aim of the current study was to understand how changes in functional and structural integrity in the brain affect the single voxel autocorrelation. In this study we examined single voxel autocorrelation and clusters of single voxel autocorrelation in patients with unilateral left and right TLE to investigate how hippocampal damage present in TLE affects the temporal signal dynamics in the hippocampus. Here, we replicated our past work (Bouffard, Golestani et al., 2023; Coughlan et al., 2023) and found that all groups demonstrated a pattern of high autocorrelation values clustered in the anterior-medial hippocampus and low autocorrelation values clustered in the posterior-lateral. There were two major findings in the TLE groups, both selective to the anterior-medial cluster. First, those with left TLE showed higher single voxel autocorrelation, suggesting a slowing down of temporal dynamics, in comparison to other groups. Second, the preservation of spatial organization of single voxel autocorrelation clusters was correlated with material-specific memory performance in both left and right TLE patients. Contrary to our predictions, we did not find significant differences in single voxel autocorrelation values or cluster preservation according to epileptogenic versus healthy hemispheres or as a function of radiologically-evident MTS. These findings suggest that single voxel autocorrelation as an index of hippocampal dynamics may be more sensitive to functional integrity than to structural integrity, at least with regards to individuals with TLE.

The first main finding was that patients with LTLE had greater single voxel autocorrelation in the anterior-medial hippocampus, indicating a slowing down of temporal dynamics, compared to controls and to patients with RTLE. This finding suggests that the single voxel autocorrelation analysis was able to detect changes to

the signal dynamics present in left TLE, and that these changes are strongest in the anterior-medial hippocampus. Other work has examined autocorrelation in the hippocampus of patients with TLE and found results different from ours. Xie et al. (2023) found reduced autocorrelation the bilateral hippocampus, suggesting more rapid dynamics across the whole hippocampus in patients with TLE, which is the opposite of our findings. There are methodological differences that could potentially account for the differences in results across studies. To compute intrinsic neural timescales, Xie et al. applied an autocorrelation function that calculated the number of temporal lags until the positive autocorrelation dropped off and became negative, resulting in an autocorrelation window that reflects the amount of time that a signal is positively correlated with itself. This method differs from the single voxel autocorrelation method used in the present study, where we applied a constant temporal window, or 2 temporal lags, applied to all voxels, resulting in a measure of signal dynamics over a fixed window of time. As there are relatively few studies examining region-specific intrinsic neural dynamics and how they are affected in cases of TLE, future work is needed to determine which signal dynamic profiles most accurately represent this population.

The second main finding was that spatial preservation of the autocorrelation clusters was predictive of memory performance. By examining cluster preservation, we were able to combine both the temporal and spatial components of autocorrelation and examine how a divergence from the norm influences memory. This finding suggests that in patients, changes in the underlying signal dynamics had subsequent effects on the single voxel autocorrelation value, which led to different cluster assignment of hippocampal voxels in patients compared to controls. This difference in cluster

assignment resulted in changes in how the autocorrelation clusters were organized throughout the hippocampus of patients which we were able to quantify with our cluster preservation measure. Here, we also showed that the more ‘normative’ the organization of autocorrelation values, particularly in the anterior-medial hippocampus, the better the memory performance in a material-specific, lateralized manner.

In previous work correlating the temporal dynamics of the BOLD signal with behavior, task-dependent changes in signal dynamics have been associated with better cognitive performance (Armbruster-Genç et al., 2016; Bouffard, Golestani et al., 2023; Protzner et al., 2013). We had predicted that our measure, single voxel autocorrelation, could be an indicator of this aspect of functional integrity and thus would be related to patient’s memory performance. This prediction was not borne out for single voxel autocorrelation values and offline memory measures. One important caveat is that we were examining single voxel autocorrelation during resting state fMRI, whereas the previous studies relating signal dynamics and behavior used task fMRI (Armbruster-Genç et al., 2016; Bouffard, Golestani et al., 2023; Garrett et al., 2011, 2014; Protzner et al., 2013). It is plausible that single voxel autocorrelation measures neural variability related to real-time cognitive processes, as seen in our past work where autocorrelation changes were related to navigation task difficulty (Bouffard, Golestani et al., 2023; Brunec, Bellana et al., 2018), but that there is a weaker relationship between single voxel autocorrelation during rest and more trait-like evaluations of behavior. Thus, chronically slower temporal dynamics may not be sufficient to explain variations in complex operations underlying offline performance on clinical memory measures. In that

sense, single voxel autocorrelation per se may not be as robust an indicator of functional integrity as measures of intrinsic connectivity (Audrain et al., 2018, 2023).

Given that we observed a relationship between cluster preservation and memory performance but did not see a relationship of single voxel autocorrelation and memory performance, it is possible that examining the temporal dynamics alone is not sufficient to explain differences in memory, and that the spatial location of the temporal dynamics is a necessary component. For example, another study that characterized location-dependent patterns of functional connectivity throughout the hippocampus in healthy controls found a continuous gradient of functional connectivity along the long axis and that individual differences in the hippocampal gradient was related to performance on a recollection task (Przeździk et al., 2019). Those results converge with the current findings and suggest that examining the temporal component of voxels (i.e., single voxel autocorrelation) might provide limited information about the functional integrity of the signal and that combining it with spatial information (i.e., cluster preservation) results in a measure that shows greater sensitivity to variations in memory performance.

Consistent with findings from our previous work (Bouffard, Golestani et al., 2023; Coughlan et al., 2023), we found that data-driven clustering of the signal voxel autocorrelation in TLE patients and controls resulted in three distinct clusters. Our clustering approach does not use a predefined number of clusters, and visual examinations of the cluster maps revealed that there were no differences in number of clusters between patients and controls, nor was there a difference between healthy and epileptogenic hemispheres. Other studies using data-driven clustering approaches of functional connectivity within the hippocampus have also found that TLE patients and

controls have a similar number of clusters to one another and a similar number of clusters in both hemispheres (Barnett et al., 2019; Voets et al., 2014). This finding suggests that the total number of autocorrelation clusters is too coarse of a metric for differentiating between patients and controls or between healthy and epileptogenic hemispheres.

We had predicted that within patients, there would be differences in single voxel autocorrelation between the healthy and epileptogenic hemispheres. We did not find support for this prediction. The lack of difference in single voxel autocorrelation between hemispheres suggests that disruptions in temporal dynamics associated with left unilateral TLE extend into both hemispheres, which is consistent with prior work that found bilateral changes to intrinsic neural timescales in patients with TLE (Xie et al., 2023). Whereas we observed a significant difference in single voxel autocorrelation between LTLE and controls, there was no difference in single voxel autocorrelation between RTLE and controls. Null findings in patients with RTLE have appeared throughout the literature, suggesting that neural changes due to TLE manifest differently in left vs. right TLE. For example, cortico-hippocampal connectivity in LTLE was predictive of post-surgery outcomes, but not in RTLE (Audrain et al., 2023; Stasenko et al., 2023). Additionally, reductions in functional connectivity between the hippocampus and DMN regions are greater in LTLE, but not RTLE (Barnett et al., 2019; Pereira et al., 2010). In the present study, hippocampal single voxel autocorrelation might be, in some part, an indication of the different connectivity profiles of left vs. right TLE. Future work is needed to characterize the changes in temporal signaling in RTLE and how it is different from LTLE.

Mesial temporal sclerosis is associated with cell loss, which is especially prominent in the anterior hippocampus. We predicted that the structural changes due to MTS would affect the autocorrelation, particularly in the anterior-medial autocorrelation cluster. Contrary to our predictions we did not find significant effects of MTS and only found a marginal trend in patients with LTLE, where patients with MTS had slightly higher single voxel autocorrelation compared to those without. We conclude that the structural changes due to MTS are separable from the neural activity that the single voxel autocorrelation measure reflects. Recent work that examined intrinsic neural timescales in the hippocampus of patients with TLE found that when accounting for structural changes in their analyses (volume and cortical thinning) there was a reduced effect size, however patients still demonstrated reduced neural timescales compared to controls (Xie et al., 2023), suggesting that autocorrelation provides information about brain function that is distinct from brain structure. It is also possible that the impact of hippocampal structural changes due to MTS are not detectable during rest, and that the effects of structural changes become more apparent during hippocampally-dependent tasks, For example, TLE-related structural changes in the hippocampus mediated the reorganization of functional memory networks during episodic retrieval states, but not during semantic retrieval states (Cabalo et al., 2023). This suggests that the impact of hippocampal structural integrity on functional memory networks might be more robust during episodic memory tasks that recruit the hippocampus.

A limitation of the current study was the resolution of the resting state data, which might have been too low to be able to isolate and exclude voxels that had cell loss. Larger voxels could obscure our ability to differentiate between voxels with and without

sclerosis, leading to the null effect of MTS. We cannot account for partial volume effects, where a single voxel might contain healthy tissue as well as CSF where sclerosis has occurred. Future work combining high resolution 7T fMRI and advanced automated hippocampal segmentation is needed to precisely quantify change in single voxel autocorrelation and relate it to structural changes caused by MTS.

5. Conclusion

By applying a fine-grained analysis of the autocorrelation of individual voxels in patients with TLE we determined that single voxel autocorrelation and autocorrelation clustering are affected by TLE. We found that in cases of left TLE there was a bilateral slowing down of neural dynamics in the anterior-medial hippocampus. We also show evidence that changes in the spatial organization of the anterior-medial autocorrelation cluster was related to verbal and visuospatial memory. This work advances our understanding of the properties of hippocampal signaling dynamics and highlights the importance of examining the spatial organization of temporal dynamics throughout the hippocampus, particularly in the anterior-medial hippocampus.

Data and Code Availability. Data and code available upon request.

Author Contributions. N.R.B., S.A., M.M., and M.P.M. contributed to the conception of the study. N.R.B. analyzed the data, prepared figures, and drafted the initial manuscript. S.A. and A.G. contributed to data preprocessing and analysis. M.P.M. provided the data

and resources needed for this experiment. All authors contributed to the revisions of the manuscript.

Declaration of Competing Interests. None of the authors has any conflict of interest to disclose.

Supplemental materials.

Reliability analysis – Overlap of individual autocorrelation clusters with group average (within-group)

We examine how reliable the spatial overlap of autocorrelation clusters was within each group. For example, for a patient with LTLE, how similar was the spatial organization of their autocorrelation clusters to all other LTLE patients. The aims of this analysis were to 1. Determine how consistent the spatial organization of autocorrelation clusters was among individuals in the same group and 2. Whether there was more variability in spatial organization of autocorrelation clusters among individuals in the LTLE and RTLE groups compared to Controls. To measure spatial overlap of autocorrelation clusters, we calculated the Jaccard coefficient between each individual's cluster map with every other individual's cluster map in their respective group (Controls, LTLE and RTLE). High spatial overlap (i.e., large Jaccard coefficients) between clusters of individuals from the same group suggests a high reliability of spatial organization of autocorrelation clusters across individuals within groups. Low spatial overlap (i.e., small Jaccard coefficients) between clusters of individuals from the same group suggests low reliability of spatial organization of autocorrelation clusters across individuals within groups. After computing the within-group Jaccard coefficients, we ran a linear mixed effects model on the within-group Jaccard coefficients with cluster (anterior-medial, intermediate, posterior-lateral), group (Controls, LTLE, RTLE), and hemisphere (left, right) as predictors.

We found a significant main effect of cluster ($F(2,355) = 6499.32$, $p < 0.001$), and a significant main effect of hemisphere ($F(1,355) = 142.50$, $p < 0.001$). We did not find a

significant main effect of group ($p = 0.183$). We also found a significant interaction between group and hemisphere ($F(2,355) = 7.60$, $p < 0.001$) and a significant interaction between cluster and hemisphere ($F(2,355) = 27.01$, $p <0.001$).

Post hoc analysis of the main effect of cluster revealed that the anterior-medial and posterior-lateral clusters had greater overlap (higher Jaccard coefficients) compared to the intermediate cluster (anterior-medial > intermediate: $t(355)=89.48$, $p <0.001$; posterior-lateral > intermediate: $t(355)=105.92$, $p < 0.001$), suggesting greater reliability of the anterior-medial cluster and posterior-lateral cluster and lower reliability of the intermediate cluster. This finding is consistent with Bouffard, Golestani, et al. (2022) and Coughlan et al. (2022), where the intermediate cluster had low reliability and was found to be inconsistent across individuals and across runs from the same individual. We also found that the posterior-lateral cluster had higher Jaccard coefficients than the anterior-medial cluster ($t(355) = 16.43$, $p < 0.001$). These results address the first aim of our analysis and conclude that the anterior-medial and posterior-lateral clusters are the most reliable clusters. Post hoc analysis of the main effect of hemisphere revealed that the right hemisphere had greater Jaccard coefficients than the left hemisphere ($t(355) = 11.93$, $p < 0.001$). This suggests that the spatial organization of clusters in the right hemisphere were more reliable among individuals of the same group than the left hemisphere.

Notably we did not find a main effect of group or any interactions with group. This result addresses the second aim of our analysis and suggests that the variability in spatial organization of autocorrelation clusters among individuals in the Control group was not significantly different from the individuals in the LTLE and RTLE groups.

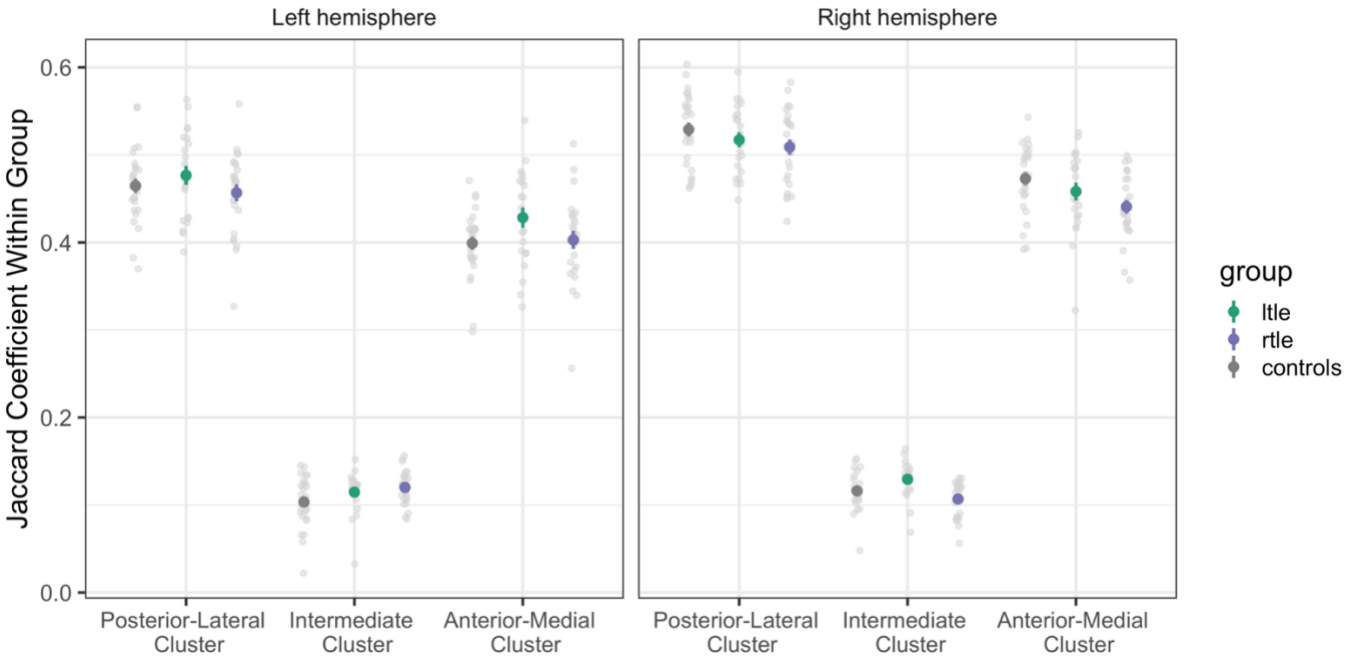

Figure S1. Autocorrelation cluster reliability – Spatial overlap of autocorrelation clusters between individuals within the same group. The Jaccard coefficient between each individual's cluster map with every other individual's cluster map in their respective group (Controls, LTLE and RTLE). High spatial overlap (i.e., large Jaccard coefficients) between clusters of individuals from the same group suggests reliable spatial organization of autocorrelation clusters across individuals within groups.

Table S1. Size of autocorrelation clusters

Group	Hemisphere	Cluster	Number of Voxels
Controls	L	Posterior-lateral	557
Controls	L	Intermediate	208
Controls	L	Anterior-medial	396
Controls	R	Posterior-lateral	540
Controls	R	Intermediate	187
Controls	R	Anterior-medial	371
LTLE	L	Posterior-lateral	554
LTLE	L	Intermediate	214
LTLE	L	Anterior-medial	393

LTLE	R	Posterior-lateral	520
LTLE	R	Intermediate	217
LTLE	R	Anterior-medial	361
RTLE	L	Posterior-lateral	548
RTLE	L	Intermediate	214
RTLE	L	Anterior-medial	399
RTLE	R	Posterior-lateral	525
RTLE	R	Intermediate	173
RTLE	R	Anterior-medial	400

Table S2. Average single voxel autocorrelation per cluster

Group	Hemisphere	MTS status	Cluster	Average Autocorrelation	SD
Controls	L	noMTS	Posterior-lateral	0.0507	0.0134
Controls	L	noMTS	Intermediate	0.0817	0.0249
Controls	L	noMTS	Anterior-medial	0.236	0.149
Controls	R	noMTS	Posterior-lateral	0.0527	0.0138
Controls	R	noMTS	Intermediate	0.0888	0.0259
Controls	R	noMTS	Anterior-medial	0.243	0.109
LTLE	L	MTS	Posterior-lateral	0.0783	0.0407
LTLE	L	MTS	Intermediate	0.13	0.0714
LTLE	L	MTS	Anterior-medial	0.365	0.208
LTLE	L	noMTS	Posterior-lateral	0.0575	0.0129
LTLE	L	noMTS	Intermediate	0.0896	0.0239
LTLE	L	noMTS	Anterior-medial	0.234	0.0981
LTLE	R	MTS	Posterior-lateral	0.0743	0.0377
LTLE	R	MTS	Intermediate	0.121	0.067
LTLE	R	MTS	Anterior-medial	0.349	0.208
LTLE	R	noMTS	Posterior-lateral	0.0604	0.0147
LTLE	R	noMTS	Intermediate	0.105	0.0319
LTLE	R	noMTS	Anterior-medial	0.291	0.12

RTLE	L	MTS	Posterior-lateral	0.0645	0.023
RTLE	L	MTS	Intermediate	0.0971	0.036
RTLE	L	MTS	Anterior-medial	0.219	0.0879
RTLE	L	noMTS	Posterior-lateral	0.0565	0.0201
RTLE	L	noMTS	Intermediate	0.0868	0.0334
RTLE	L	noMTS	Anterior-medial	0.185	0.0716
RTLE	R	MTS	Posterior-lateral	0.0621	0.0198
RTLE	R	MTS	Intermediate	0.0999	0.0351
RTLE	R	MTS	Anterior-medial	0.24	0.151
RTLE	R	noMTS	Posterior-lateral	0.0584	0.0146
RTLE	R	noMTS	Intermediate	0.0912	0.0238
RTLE	R	noMTS	Anterior-medial	0.22	0.0756

Table S3. Correlation between average autocorrelation and memory performance

Group	Hemisphere	Cluster	Verbal Memory (R)	P value
LTLE	Left	Posterior-lateral	-0.336	0.12
LTLE	Left	Anterior-medial	-0.0988	0.65
LTLE	Right	Posterior-lateral	-0.346	0.11
LTLE	Right	Anterior-medial	-0.205	0.35
Group	**Hemisphere**	**Cluster**	**Visuospatial Memory (R)**	**P value**
RTLE	Left	Posterior-lateral	0.0674	0.75
RTLE	Left	Anterior-medial	-0.157	0.45
RTLE	Right	Posterior-lateral	0.114	0.59
RTLE	Right	Anterior-medial	-0.133	0.53

Table S4. Cluster preservation (Jaccard coefficients) for each autocorrelation cluster

Group	Hemisphere	MTS status	Cluster	Jaccard coefficient	SD
LTLE	L	MTS	Posterior-lateral	0.495	0.0696
LTLE	L	MTS	Anterior-medial	0.428	0.107
LTLE	L	noMTS	Posterior-lateral	0.479	0.0451
LTLE	L	noMTS	Anterior-medial	0.418	0.0762
LTLE	R	MTS	Posterior-lateral	0.517	0.0433
LTLE	R	MTS	Anterior-medial	0.503	0.0717
LTLE	R	noMTS	Posterior-lateral	0.507	0.0426
LTLE	R	noMTS	Anterior-medial	0.482	0.0844
RTLE	L	MTS	Posterior-lateral	0.466	0.0603
RTLE	L	MTS	Anterior-medial	0.41	0.0978
RTLE	L	noMTS	Posterior-lateral	0.488	0.0232
RTLE	L	noMTS	Anterior-medial	0.426	0.101
RTLE	R	MTS	Posterior-lateral	0.493	0.0468
RTLE	R	MTS	Anterior-medial	0.472	0.0808
RTLE	R	noMTS	Posterior-lateral	0.516	0.0454
RTLE	R	noMTS	Anterior-medial	0.486	0.08

Reference

Armbruster-Genç, D. J. N., Ueltzhöffer, K., & Fiebach, C. J. (2016). Brain Signal Variability Differentially Affects Cognitive Flexibility and Cognitive Stability. *The Journal of Neuroscience*, *36*(14), 3978–3987. https://doi.org/10.1523/JNEUROSCI.2517-14.2016

Audrain, S., Barnett, A. J., & McAndrews, M. P. (2018). Language network measures at rest indicate individual differences in naming decline after anterior temporal lobe resection. *Human Brain Mapping*, *39*(11), 4404–4419.

Audrain, S., Barnett, A., Mouseli, P., & McAndrews, M. P. (2023). Leveraging the resting brain to predict memory decline after temporal lobectomy. *Epilepsia*, epi.17767. https://doi.org/10.1111/epi.17767

Barnett, A. J., Man, V., & McAndrews, M. P. (2019). Parcellation of the Hippocampus Using Resting Functional Connectivity in Temporal Lobe Epilepsy. *Frontiers in Neurology*, *10*, 920. https://doi.org/10.3389/fneur.2019.00920

Behzadi, Y., Restom, K., Liau, J., & Liu, T. T. (2007). A component based noise correction method (CompCor) for BOLD and perfusion based fMRI. *Neuroimage*, *37*(1), 90–101.

Bernasconi, N., Bernasconi, A., Caramanos, Z., Antel, S. B., Andermann, F., & Arnold, D. L. (2003). Mesial temporal damage in temporal lobe epilepsy: A volumetric MRI study of the hippocampus, amygdala and parahippocampal region. *Brain*, *126*, 462–469. https://doi.org/10.1093/brain/awg034

Bernhardt, B. C., Bernasconi, A., Liu, M., Hong, S.-J., Caldairou, B., Goubran, M., Guiot, M. C., Hall, J., & Bernasconi, N. (2016). The spectrum of structural and

functional imaging abnormalities in temporal lobe epilepsy. *Annals of Neurology*, *80*(1), 142–153.

Blondel, V. D., Guillaume, J.-L., Lambiotte, R., & Lefebvre, E. (2008). Fast unfolding of communities in large networks. *Journal of Statistical Mechanics: Theory and Experiment*, *2008*(10), P10008.

Bollmann, S., Puckett, A. M., Cunnington, R., & Barth, M. (2018). Serial correlations in single-subject fMRI with sub-second TR. *NeuroImage*, *166*, 152–166.

Bouffard, N. R., Golestani, A., Brunec, I. K., Bellana, B., Park, J. Y., Barense, M. D., & Moscovitch, M. (2023). Single voxel autocorrelation uncovers gradients of temporal dynamics in the hippocampus and entorhinal cortex during rest and navigation. *Cerebral Cortex*, *33*(6), 3265–3283. https://doi.org/10.1093/cercor/bhac480

Brunec, I. K., Bellana, B., Ozubko, J. D., Man, V., Robin, J., Liu, Z.-X., Grady, C., Rosenbaum, R. S., Winocur, G., Barense, M. D., & Moscovitch, M. (2018). Multiple Scales of Representation along the Hippocampal Anteroposterior Axis in Humans. *Current Biology*, *28*(13), 2129-2135.e6. https://doi.org/10.1016/j.cub.2018.05.016

Cabalo, D. G., Dekraker, J., Royer, J., Xie, K., Tavakol, S., Rodriguez-Cruces, R., Bernasconi, A., Bernasconi, N., Weil, A., Pana, R., Frauscher, B., Caciagli, L., Jefferies, E., Smallwood, J., & Bernhardt, B. (2023). *Differential Reorganization of Episodic and Semantic Memory Systems in Epilepsy-Related Mesiotemporal Pathology* [Preprint]. Neuroscience. https://doi.org/10.1101/2023.09.28.560002

Coras, R., & Blümcke, I. (2015). Clinico-pathological subtypes of hippocampal sclerosis in temporal lobe epilepsy and their differential impact on memory impairment. *Neuroscience*, *309*, 153–161. https://doi.org/10.1016/j.neuroscience.2015.08.003

Coughlan, G., Bouffard, N. R., Golestani, A., Thakral, P. P., Schacter, D. L., Grady, C., & Moscovitch, M. (2023). Transcranial magnetic stimulation to the angular gyrus modulates the temporal dynamics of the hippocampus and entorhinal cortex. *Cerebral Cortex*, *33*(6), 3255–3264. https://doi.org/10.1093/cercor/bhac273

Garrett, D. D., Kovacevic, N., McIntosh, A. R., & Grady, C. L. (2011). The Importance of Being Variable. *The Journal of Neuroscience*, *31*(12), 4496–4503. https://doi.org/10.1523/JNEUROSCI.5641-10.2011

Garrett, D. D., McIntosh, A. R., & Grady, C. L. (2014). Brain Signal Variability is Parametrically Modifiable. *Cerebral Cortex*, *24*(11), 2931–2940. https://doi.org/10.1093/cercor/bht150

Jackson, G. D., Berkovic, S. F., Tress, B., Kalnins, R. M., Fabinyi, G., & Bladin, P. F. (1990). Hippocampal sclerosis can be reliably detected by magnetic resonance imaging. *Neurology*, *40*(12), 1869–1869.

Kelley, W. M., Miezin, F. M., McDermott, K. B., Buckner, R. L., Raichle, M. E., Cohen, N. J., Ollinger, J. M., Akbudak, E., Conturo, T. E., Snyder, A. Z., & others. (1998). Hemispheric specialization in human dorsal frontal cortex and medial temporal lobe for verbal and nonverbal memory encoding. *Neuron*, *20*(5), 927–936.

Kim, H., Yi, S., Son, E. I., & Kim, J. (2003). Material-specific memory in temporal lobe epilepsy: Effects of seizure laterality and language dominance. *Neuropsychology*, *17*(1), 59.

Kuzniecky, R., Bilir, E., Gilliam, F., Faught, E., Palmer, C., Morawetz, R., & Jackson, G. (1997). Multimodality MRI in mesial temporal sclerosis: Relative sensitivity and specificity. *Neurology*, *49*(3), 774–778.

Monto, S., Vanhatalo, S., Holmes, M. D., & Palva, J. M. (2007). Epileptogenic neocortical networks are revealed by abnormal temporal dynamics in seizure-free subdural EEG. *Cerebral Cortex*, *17*(6), 1386–1393.

Parish, L., Worrell, G., Cranstoun, S., Stead, S., Pennell, P., & Litt, B. (2004). Long-range temporal correlations in epileptogenic and non-epileptogenic human hippocampus. *Neuroscience*, *125*(4), 1069–1076.

Pereira, F. R. S., Alessio, A., Sercheli, M. S., Pedro, T., Bilevicius, E., & Rondina, J. M. (2010). Asymmetrical hippocampal connectivity in mesial temporal lobe epilepsy: Evidence from resting state fMRI. *BMC Neurosci*, *11*(1).

Protzner, A. B., Kovacevic, N., Cohn, M., & McAndrews, M. P. (2013). Characterizing Functional Integrity: Intraindividual Brain Signal Variability Predicts Memory Performance in Patients with Medial Temporal Lobe Epilepsy. *Journal of Neuroscience*, *33*(23), 9855–9865. https://doi.org/10.1523/JNEUROSCI.3009-12.2013

Protzner, A. B., Valiante, T., Kovacevic, N., McCormick, C., & McAndrews, M. P. (2010). Hippocampal signal complexity in mesial temporal lobe epilepsy: A noisy brain is a healthy brain. *Archives Italiennes de Biologie*, *148*(3), 289–297.

Przeździk, I., Faber, M., Fernández, G., Beckmann, C. F., & Haak, K. V. (2019). The functional organisation of the hippocampus along its long axis is gradual and

predicts recollection. *Cortex*, *119*, 324–335. https://doi.org/10.1016/j.cortex.2019.04.015

Raut, R. V., Snyder, A. Z., & Raichle, M. E. (2020). Hierarchical dynamics as a macroscopic organizing principle of the human brain. *Proceedings of the National Academy of Sciences*, *117*(34), 20890–20897. https://doi.org/10.1073/pnas.2003383117

Sinclair, A. H., Manalili, G. M., Brunec, I. K., Adcock, R. A., & Barense, M. D. (2020). *Prediction Errors Disrupt Hippocampal Representations and Update Episodic Memories* [Preprint]. Neuroscience. https://doi.org/10.1101/2020.09.29.319418

Stasenko, A., Kaestner, E., Arienzo, D., Schadler, A. J., Helm, J. L., Shih, J. J., Ben-Haim, S., & McDonald, C. R. (2023). Preoperative white matter network organization and memory decline after epilepsy surgery. *Journal of Neurosurgery*, 1–12. https://doi.org/10.3171/2023.4.JNS23347

St-Laurent, M., McCormick, C., Cohn, M., Mišić, B., Giannoylis, I., & McAndrews, M. P. (2014). Using multivariate data reduction to predict postsurgery memory decline in patients with mesial temporal lobe epilepsy. *Epilepsy & Behavior*, *31*, 220–227. https://doi.org/10.1016/j.yebeh.2013.09.043

Thom, M., Liagkouras, I., Martinian, L., Liu, J., Catarino, C. B., & Sisodiya, S. M. (2012). Variability of sclerosis along the longitudinal hippocampal axis in epilepsy: A post mortem study. *Epilepsy Research*, *102*(1–2), 45–59.

Voets, N. L., Zamboni, G., Stokes, M. G., Carpenter, K., Stacey, R., & Adcock, J. E. (2014). Aberrant Functional Connectivity in Dissociable Hippocampal Networks Is

Associated with Deficits in Memory. *The Journal of Neuroscience*, *34*(14), 4920–4928. https://doi.org/10.1523/JNEUROSCI.4281-13.2014

Whitfield-Gabrieli, S., & Nieto-Castanon, A. (2012). Conn: A functional connectivity toolbox for correlated and anticorrelated brain networks. *Brain Connect*, *2*, 125–141. https://doi.org/10.1089/brain.2012.0073

Wickramaarachchi, C., Frincu, M., Small, P., & Prasanna, V. K. (2014). Fast parallel algorithm for unfolding of communities in large graphs. *2014 IEEE High Performance Extreme Computing Conference (HPEC)*, 1–6.

Wolff, A., Berberian, N., Golesorkhi, M., Gomez-Pilar, J., Zilio, F., & Northoff, G. (2022). Intrinsic neural timescales: Temporal integration and segregation. *Trends in Cognitive Sciences*, *26*(2), 159–173. https://doi.org/10.1016/j.tics.2021.11.007

Xie, K., Royer, J., Lariviere, S., Rodriguez-Cruces, R., de Wael, R. V., Park, B., Auer, H., Tavakol, S., DeKraker, J., Abdallah, C., Caciagli, L., Bassett, D. S., Bernasconi, A., Bernasconi, N., Frauscher, B., Concha, L., & Bernhardt, B. C. (2023). Atypical intrinsic neural timescales in temporal lobe epilepsy. *Epilepsia*, *64*(4), 998–1011. https://doi.org/10.1111/epi.17541